

**Figure 3.** Development of tumors in livers receiving hepatic progenitor cells from AID Tg mice. (a) Macroscopic images of tumors that developed in recipient mice receiving progenitor cells from AID Tg mice. (b) Microscopic images of a liver tumor that developed in a recipient mouse receiving hepatic progenitor cells from an AID Tg mouse. Upper, AFP-positive part; Middle, CK19-positive part; Lower, non-tumorous liver tissue. Immunohistochemical staining for H&E, AFP and CK19 are shown. (c) Southern blot analysis for the AID transgene. DNA was extracted from three liver tumor tissues (Tumor #1, 2, 3), a non-tumor liver tissue (Non-tumor), the kidney of the corresponding animal, a liver of a TRECK mouse (Negative control; NC) and a liver of an AID Tg mouse (Positive control; PC), followed by the amplification and hybridization to the probe specific for the AID transgene. (d) Results of quantitative genomic PCR for AID transgene in three liver tumor tissues, a non-tumor liver tissue and the kidney of the corresponding animal. N.D. means not detected.

To examine whether the cancers that developed in recipient mice liver were derived from the transplanted hepatic progenitor cells, we examined the expression of the AID Tg mice-specific transgene in three randomly selected tumors that developed in the recipient livers. Southern blotting analyses revealed strong signals of the AID transgene in the tumor tissues (Fig. 3c). Weak signal of the AID transgene was also detected in the non-tumorous region, suggesting

continuous engraftment of the transplanted hepatic progenitor-derived cells in the recipient mouse liver. In contrast, there were no detectable signals of the AID transgene in organs other than the liver of recipient mice, such as kidney, or in liver tissues of the TRECK mice without receiving the transplantation. Quantitative genomic PCR analyses also confirmed that all tumor tissues examined strongly expressed the AID transgene (Fig. 3d). Moreover, the expression level of hHB-EGF in the tumor tissue was significantly lower than that in the surrounding non-tumorous liver tissue (Supporting Information Fig. 2c). These findings suggested that the transplanted hepatic progenitor cells with constitutive AID expression achieved the malignant transformation and progressed to either HCC or cholangiocarcinoma.

#### Landscape of genetic alterations accumulated in the transplanted hepatic progenitor cells during the process of malignant transformation

To unveil the landscape of genetic alterations that accumulated in the transplanted hepatic progenitor cells during the process of tumorigenesis, we determined the sequences of the whole exome in two independent liver cancers from two different recipient mice and the corresponding hepatic progenitor cells of the same AID Tg mice from which they originated (Table 1). As a control, we also determined the whole exome sequences of the livers of their littermates with a wild-type phenotype. A total of 94.2% of the reads were properly aligned to the reference mouse genome and accordingly we obtained about 4.4 Gb of the aligned sequence data per sample on average after exome enrichment. 77.6% of the captured target exons were covered by 20 $\times$  or more coverage depth read with a high quality genotype call. The variant filtering process is summarized in Supporting Information Figure 1. We identified 24 [23 single nucleotide variants (SNVs) and one indel] and 162 (160 SNVs and two indels) somatic mutations in HCC#1 and HCC#2, of which the number of mutated genes with SNVs were 23 (HCC#1) and 105 (HCC#2), respectively (Table 2, and Supporting Information Table 4). As shown in Supporting Information Figure 2d, C/G to T/A substitution pattern was dominant, consistent with the previous finding that AID induces C/G to T/A transition into the genome.<sup>23,24</sup> The candidate variants were then validated by conventional direct population Sanger sequencing (Supporting Information Fig. 3), and we finally confirmed that 20 (HCC#1) and 87 (HCC#2) SNVs were non-synonymous variants. Among them, there were no genes commonly mutated in both tumors. Interestingly, 19 of 23 (82.6% in HCC#1) and 80 of 105 (76.2% in HCC #2) genes with SNVs were those reported in human liver cancer tissues (International Cancer Genome Consortium: <http://www.icgc.org/>). Although tumor-suppressor Trp 53 gene also acquired mutations in both tumors, the nucleotide alteration rate was less than 20%. Pathway analyses using the KEGG (Kyoto Encyclopedia of Genes and Genomes) database (<http://www.genome.jp/kegg/>) revealed that 11 (HCC#1) and

**Table 1.** Overview of exome sequencing data

	Wild-type liver	HPCs	HCC #1	HCC #2
Total reads	40,531,478	66,249,904	74,974,839	71,744,206
Aligned reads	39,836,233	64,288,711	73,520,622	70,334,812
Aligned sequence (bp)	2,895,739,984	4,640,585,570	5,299,669,630	4,893,614,870
Median read depth	47	69	83	69
1× coverage	26,389,043	26,497,041	26,651,266	26,676,550
8× coverage	25,737,539	25,954,163	26,050,816	25,993,659
20× coverage	24,034,052	25,453,341	25,554,806	25,105,923
30× coverage	21,708,378	24,777,302	24,956,955	23,893,453

Whole exome sequencing were performed for the liver of wild-type mouse, the hepatic progenitor cells (HPCs) of the AID Tg mouse, and liver cancer tissues (HCC#1 and HCC#2) developed in the two different TRECK mice transplanted with HPCs. Total reads, aligned reads, aligned sequence(bp), median read depth and the number of the captured target exons which were 1×, 8×, 20× and 30× or more coverage depth read were shown for each sample.

Abbreviations: HCC: hepatocellular carcinoma; HPC: hepatic progenitor cell.

**Table 2.** Characteristics of single nucleotide variants (SNVs) identified in the liver cancers derived from the hepatic progenitor cells of the AID Tg mice

	HCC#1	HCC#2
Number of SNVs (single nucleotide variants)	23	160
Number of mutated genes with SNVs	23	105
Number of SNVs with nonsynonymous variants	20 of 23 (86.7%)	87 of 160 (54.3%)
Number of mutated genes with SNVs reported in human liver cancer tissues	19 of 23 (82.6%)	80 of 105 (76.2%)
Number of mutated genes with SNVs categorized into well-known pathways in KEGG	11 of 23 (47.8%)	66 of 105 (62.8%)
Number of mutated genes with SNVs highly expressed in fetal or adult liver relative to bone marrow	21 of 22 <sup>1</sup> (95.4%)	85 of 99 <sup>1</sup> (85.8%)

<sup>1</sup>Genes that were not present in the microarray panel were excluded from the analysis.

Abbreviations: KEGG: Kyoto Encyclopedia of Genes and Genomes; SNV: single nucleotide variant.

66 (HCC#2) genes were categorized into the well-known signaling pathways, including peroxisome proliferator-activated receptor (PPAR) and mitogen-activated protein kinase (MAPK) signaling, and cell adhesion function (Table 3).

Although it is widely recognized that the mutational profiles of the tumor-related genes differ between different tissues, the mechanisms of those organ-specific differences in the mutated genes during the process of tumorigenesis remain unclear. We speculated that the genes that acquired mutations in HCC tissues might be preferentially and actively transcribed in hepatic lineage cells, because it has been shown that AID-induced mutagenic activity is directly proportional to the transcription levels of the target gene.<sup>35–37</sup> Therefore, we analyzed the gene expression profiles in the fetal and adult liver using microarray, and examined whether the mutated genes in HCC tissues were transcribed at relatively higher levels in liver-lineage cells compared with hematopoietic lineage cells. Among the mutated genes identified, transcription levels of 95.4% and 85.8% of the genes in HCC#1 and HCC#2, respectively, were higher in fetal and/or adult liver tissues than in bone marrow-derived hematopoietic cells (Table 2, and Supporting Information Table 4), indicating

that the genes actively transcribed in fetal and/or adult liver cells might have preferentially acquired the mutations through the genotoxic activity of AID. Consistently, quantitative RT-PCR analyses revealed that all the mutated genes analyzed were actively transcribed in adult liver tissues (Supporting Information Fig. 4). In contrast, representative genes that are actively transcribed in hematopoietic tissues,<sup>38</sup> such as *Cd4*, *Cd5* and *Tgfb $\beta$ 2*, showed no mutations in liver tumors and less or no transcription in the liver compared with other organs (Supporting Information Fig. 4). We also confirmed that 19 (82.6% in HCC#1) and 93 (88.6% in HCC#2) of the mutated genes were actively transcribed in the liver tissues based on the mouse whole transcriptome analysis.<sup>39</sup> Together, these findings suggest that the acquisition of mutations during hepatocarcinogenesis strongly depends on the transcription of target genes in the liver-lineage cells.

## Discussion

Recently, recognition of the role of tissue stem/progenitor cells in the carcinogenesis process led to a new hypothesis that cancer arises from tissue stem/progenitor cells.<sup>40</sup> Indeed,

Table 3. Categorization of the mutated genes in HCCs using the KEGG (Kyoto encyclopedia of genes and Genomes) database

HCC#1				
Insulin signaling pathway (2)	Sorbs1	Prkar1b		
Pathways in cancer (2)	Stk36	ErbB2		
Adherens junction (2)	Sorbs1	ErbB2		
HCC#2				
Metabolic pathways (12)	Akr1c6	Dgat2	Sephs2	Chka
	Cyp2e1	Maob	Nt5e	Pck1
	Rdh8	St3gal6	Tk1	Tkt
PPAR signaling pathway (7)	Fads2	Slc27a2	Apoa1	Apoa2
	Fabp5	Pck1	Scd1	
MAPK signaling pathway (6)	Jun	Jund	Fos	
	Dusp4	Rac3	Gadd45g	
Pathways in cancer (6)	Jun	Nfkbia	Ceppa	
	Fzd7	Rac3	Fos	
	Jun	Nfkbia	Fos	
Toll-like receptor signaling pathway (3)	Jun	Nfkbia	Fos	
Hepatitis C (3)	Ldlr	Nfkbia	Socs3	
Adipocytokine signaling pathway (3)	Nfkbia	Pck1	Socs3	
Wnt signaling pathway (3)	Fzd7	Jun	Rac3	

Values in parenthesis show the number of the genes categorized into each pathway.

Abbreviations: MAPK: mitogen-activated protein kinase; PPAR: peroxisome proliferator-activated receptor.

genetically-engineered fetal progenitor cells lacking the tumor-suppressor gene function have been shown to play a role as the origin of liver cancer.<sup>9,11,41</sup> Whether the stepwise accumulation of genetic alterations on hepatic stem/progenitor cells contributes to the development of tumor cells, however, remains unknown. In our study, we demonstrated that engrafted hepatic progenitor cells originated from the AID Tg mice progressed to liver tumors, including both HCC and cholangiocarcinoma, through the accumulation of somatic mutations in a variety of target genes.

Several previous studies demonstrated that the transplanted putative fetal liver stem/progenitor cells are capable of repopulating the liver that encounter extensive liver injury favoring the proliferation and survival of transplanted hepatocytes.<sup>42-44</sup> The DT receptor has been identified as a membrane-anchored form of the HB-EGF precursor.<sup>26</sup> Recently, it was shown that transplanted hepatic progenitor cells derived from the fetal liver were efficiently engrafted and repopulated in the liver of recipient HB-EGF-expressing mice with DT stimulation.<sup>27,28</sup> Using this model, efficient engraftment of the transplanted cells in recipient mice with HB-EGF expression in the liver enabled us to examine the fate of transplanted hepatic progenitor cells with constitutive AID expression. Notably, liver tumors with histologic features of human HCC developed in the recipient mice that received the hepatic progenitor cells derived from the AID Tg mice, while no tumorigenesis was observed in the recipient mice transplanted with hepatic progenitor cells of control mice.

The findings that the tumors contained the AID transgene indicated that these tumors were derived from the transplanted hepatic progenitor cells accompanied with the AID-induced genetic aberrations. Interestingly, one of those tumors showed both the characteristics of HCC and cholangiocarcinoma in a single nodule, suggesting that the hepatic progenitor cells with the accumulation of genetic aberration could possess the potential to progress both HCC- and cholangiocarcinoma-lineage tumor cells. Alternatively, it might be possible that AID-mediated genetic alterations contribute to modifying the differentiation status of tumor cells, leading to either HCC or bile duct cancers from common progenitor cells.

Sequencing of whole genomes, whole exomes and whole transcriptomes of cancer samples has recently become feasible using deep sequencing technologies. In this study, to obtain the overall picture of genetic alterations accumulated in the hepatic progenitor cells of the AID Tg mice that achieved malignant transformation, we performed whole exome sequencing of the transplanted progenitor cells and the resultant tumor tissues, and unveiled the landscape of genetic alterations that accumulated during tumorigenesis. We found that various genetic aberrations, mainly SNVs, were highly accumulated in the tumors, further supporting the putative involvement of aberrant AID activity in the development of HCC. One thing to be noted is that approximately 80% of mutated genes detected in the liver cancer tissues developed in the recipient mice have been reported to

be mutated in human HCC tissues (International Cancer Genome Consortium; <http://www.icgc.org/>), although it is not possible to draw a definitive conclusion from analyses of the limited number of HCCs that developed in the recipient mice. Functional annotation analyses revealed that many of the genes that acquired genetic aberrations are categorized into several important signaling pathways, including those involved in the regulation of cell proliferation, cell metabolism and cell adhesion. Thus, it could be suggested the step-wise dysregulation of cell function caused by the accumulation of genetic aberrations in hepatic progenitor cells appears to play a pivotal role in the development of tumor cells.

We previously revealed that genetic changes induced by the genotoxic activity of AID show organ-specific profiles and suggested the possibility that the target preference of AID-induced mutagenesis contributes to the diversity of tissue-specific oncogenic pathways.<sup>23</sup> One possible explanation for the target selection for mutagenesis is that AID preferentially induces mutations in the actively transcribed genes in each cell, because AID likely induces somatic mutations on the single-strand DNA exposed during the transcription process.<sup>35–37</sup> Consistent with this hypothesis, we confirmed in this study that the majority of genes with SNVs were the actively transcribed genes in liver-lineage cells. However, we also observed that the transcription level of the gene is not solely responsible for the acquisition of AID-mediated genotoxicity, because one of the most actively transcribed hepatotrophic genes, albumin, did not accumulate SNVs in liver tumor cells (data not shown). Consistently, extensive sequencing of various genes in B lymphocytes revealed that only 25% of the transcribed genes accumulated SNVs in an AID-dependent manner.<sup>45</sup> Mutational hotspots preferentially attacked by AID genotoxicity frequently possess unique

sequence characteristics, so-called RGYW/WRCY motifs (where W = A or T, R = A or G and Y = C or T) in transcribed targets.<sup>46</sup> Moreover, a recent study reported clusters of various types of repeat sequences in the vicinity of cleaved sites in AID target genes.<sup>47</sup> Thus, target selection of AID-mediated mutagenesis might require both active transcription and sequence characteristics of the genes.

In conclusion, the findings in our study suggested that mutagenic activity of AID might contribute to the malignant transformation of hepatic progenitor cells to liver cancer cells via the induction of genetic alterations. Some of the actively transcribed genes in the liver-lineage cells preferentially accumulated SNVs and might contribute to the development of tumor cells. However, based on the model used in our study, we could not fully determine whether the developed tumors derived directly from the fetal hepatic progenitor cells or via mature hepatocytes, because the transplanted fetal progenitor cells differentiated into mature hepatocytes in the recipient liver.<sup>27</sup> Moreover, the truly significant driver mutations responsible for hepatocarcinogenesis remain unclear. Thus, further elucidation of the precise step of the AID-induced accumulation of genetic aberrations will be required to identify the genetic alterations that possess the key to the carcinogenesis process. In addition, the fractionation by fluorescence-activated cell sorting would be essential to identify the subset of hepatic stem/progenitor cells that play a role in the origin of tumor cells.

#### Acknowledgements

The authors are grateful for the support of Research Fellowships of the Japan Society for the Promotion of Science (JSPS) for Young Scientists. They thank Dr. I. Ikai, Dr. T. Machimoto and Dr. R. Kamimura for helpful suggestion and Dr. K. Terasawa, Dr. Y. Fujii, Ms. K. Matsubara and Ms. C. Kakimoto for help with the analyses.

#### References

- Hanahan D, Weinberg RA. The hallmarks of cancer. *Cell* 2000;100:57–70.
- Thorgeirsson SS, Grisham JW. Molecular pathogenesis of human hepatocellular carcinoma. *Nat Genet* 2002;31:339–46.
- Hussain SP, Schwank J, Staib F, et al. TP53 mutations and hepatocellular carcinoma: insights into the etiology and pathogenesis of liver cancer. *Oncogene* 2007;26:2166–76.
- Guichard C, Amadio G, Imbeaud S, et al. Integrated analysis of somatic mutations and focal copy-number changes identifies key genes and pathways in hepatocellular carcinoma. *Nat Genet* 2012;44:694–8.
- Reya T, Morrison SJ, Clarke MF, et al. Stem cells, cancer, and cancer stem cells. *Nature* 2001;414:105–11.
- Pardoll R, Clarke MF, Morrison SJ. Applying the principles of stem-cell biology to cancer. *Nat Rev Cancer* 2003;3:895–902.
- Burkert J, Wright NA, Alison MR. Stem cells and cancer: an intimate relationship. *J Pathol* 2006;209:287–97.
- Mishra L, Banker T, Murray J, et al. Liver stem cells and hepatocellular carcinoma. *Hepatology* 2009;49:318–29.
- Dumble ML, Croager EJ, Yeoh GCT, et al. Generation and characterization of p53 null transgenic hepatic progenitor cells: oval cells give rise to hepatocellular carcinoma. *Carcinogenesis* 2002;23:435–45.
- Zender L, Spector MS, Xue W, et al. Identification and validation of oncogenes in liver cancer using an integrative oncogenomic approach. *Cell* 2006;125:1253–67.
- Xue W, Zender L, Miething C, et al. Senescence and tumour clearance is triggered by p53 restoration in murine liver carcinomas. *Nature* 2007;445:656–60.
- Yamashita T, Li J, Budhu A, et al. EpCAM-positive hepatocellular carcinoma cells are tumor-initiating cells with stem/progenitor cell features. *Gastroenterology* 2009;136:1012–24.
- Durnez A, Verslype C, Nevens F, et al. The clinicopathological and prognostic relevance of cytokeratin 7 and 19 expression in hepatocellular carcinoma. A possible progenitor cell origin. *Histopathology* 2006;49:138–51.
- Roskams T. Liver stem cells and their implication in hepatocellular and cholangiocarcinoma. *Oncogene* 2006;25:3818–22.
- Komuta M, Spec B, Vander Borgh S, et al. Clinicopathological study on cholangiolocellular carcinoma suggesting hepatic progenitor cell origin. *Hepatology* 2008;47:1544–56.
- Tang Y, Kitisin K, Jogunoori W, et al. Progenitor/stem cells give rise to liver cancer due to aberrant TGF-beta and IL-6 signaling. *Proc Natl Acad Sci U S A* 2008;105:2445–50.
- Muramatsu M, Kinoshita K, Fagarasan S, et al. Class switch recombination and hypermutation require activation-induced cytidine deaminase (AID), a potential RNA editing enzyme. *Cell* 2000;102:553–63.
- Honjo T, Kinoshita K, Muramatsu M. Molecular mechanism of class switch recombination: linkage with somatic hypermutation. *Annu Rev Immunol* 2002;20:165–96.
- Matsumoto Y, Marusawa H, Kinoshita K, et al. Helicobacter pylori infection triggers aberrant

- expression of activation-induced cytidine deaminase in gastric epithelium. *Nat Med* 2007;13:470–6.
20. Endo Y, Marusawa H, Kou T, et al. Activation-induced cytidine deaminase links between inflammation and the development of colitis-associated colorectal cancers. *Gastroenterology* 2008;135:889–98.
  21. Endo Y, Marusawa H, Kinoshita K, et al. Expression of activation-induced cytidine deaminase in human hepatocytes via NF-kappaB signaling. *Oncogene* 2007;26:5587–95.
  22. Kou T, Marusawa H, Kinoshita K, et al. Expression of activation-induced cytidine deaminase in human hepatocytes during hepatocarcinogenesis. *Int J Cancer* 2007;120:469–76.
  23. Chiba T, Marusawa H, Ushijima T. Inflammation-associated cancer development in digestive organs: mechanisms and roles for genetic and epigenetic modulation. *Gastroenterology* 2012;143:550–63.
  24. Okazaki IM, Hiai H, Kakazu N, et al. Constitutive expression of AID leads to tumorigenesis. *J Exp Med* 2003;197:1173–81.
  25. Morisawa T, Marusawa H, Ueda Y, et al. Organ-specific profiles of genetic changes in cancers caused by activation-induced cytidine deaminase expression. *Int J Cancer* 2008;123:2735–40.
  26. Saito M, Iwakaki T, Tayu C, et al. Diphtheria toxin receptor-mediated conditional and targeted cell ablation in transgenic mice. *Nat Biotechnol* 2001;19:746–50.
  27. Machimoto T, Yasuchika K, Komori J, et al. Improvement of the survival rate by fetal liver cell transplantation in a mice lethal liver failure model. *Transplantation* 2007;84:1233–9.
  28. Ishii T, Yasuchika K, Machimoto T, et al. Transplantation of embryonic stem cell-derived endodermal cells into mice with induced lethal liver damage. *Stem cells* 2007;25:3252–60.
  29. Nasu A, Marusawa H, Ueda Y, et al. Genetic heterogeneity of hepatitis C virus in association with antiviral therapy determined by ultra-deep sequencing. *PLoS One* 2011;6:e24907.
  30. Fujiwara M, Marusawa H, Wang HQ, et al. Parkin as a tumor suppressor gene for hepatocellular carcinoma. *Oncogene* 2008;27:6002–11.
  31. Ishii T, Yasuchika K, Fujii H, et al. In vitro differentiation and maturation of mouse embryonic stem cells into hepatocytes. *Exp Cell Res* 2005;309:68–77.
  32. Nakatani T, Mizuhara E, Minaki Y, et al. Helt, a novel basic-helix-loop-helix transcriptional repressor expressed in the developing central nervous system. *J Biol Chem* 2004;279:16356–67.
  33. Toda Y, Kono K, Abiru H, et al. Application of tyramide signal amplification system to immunohistochemistry: a potent method to localize antigens that are not detectable by ordinary method. *Pathol Int* 1999;49:479–83.
  34. Yasuchika K, Hirose T, Fujii H, et al. Establishment of a highly efficient gene transfer system for mouse fetal hepatic progenitor cells. *Hepatology* 2002;36:1488–97.
  35. Yoshikawa K, Okazaki IM, Eto T, et al. AID enzyme-induced hypermutation in an actively transcribed gene in fibroblasts. *Science* 2002;296:2033–6.
  36. Chaudhuri J, Tian M, Khuong C, et al. Transcription-targeted DNA deamination by the AID antibody diversification enzyme. *Nature* 2003;422:726–30.
  37. Ramiro AR, Stavropoulos P, Jankovic M, et al. Transcription enhances AID-mediated cytidine deamination by exposing single-stranded DNA on the nontemplate strand. *Nat Immunol* 2003;4:452–6.
  38. Kotani A, Okazaki IM, Muramatsu M, et al. A target selection of somatic hypermutations is regulated similarly between T and B cells upon activation-induced cytidine deaminase expression. *Proc Natl Acad Sci U S A* 2005;102:4506–11.
  39. Mortazavi A, Williams BA, McCue K, et al. Mapping and quantifying mammalian transcriptomes by RNA-Seq. *Nat Methods* 2008;5:621–8.
  40. Sell S, Leffert HL. Liver cancer stem cells. *J Clin Oncol* 2008;26:2800–5.
  41. Katz SF, Lechel A, Obenauf AC, et al. Disruption of Trp53 in livers of mice induces formation of carcinomas with bilineal differentiation. *Gastroenterology* 2012;142:1229–39.
  42. Nierhoff D, Ogawa A, Oertel M, et al. Purification and characterization of mouse fetal liver epithelial cells with high in vivo repopulation capacity. *Hepatology* 2005;42:130–9.
  43. Oertel M, Menthena A, Chen YQ, et al. Purification of fetal liver stem/progenitor cells containing all the repopulation potential for normal adult rat liver. *Gastroenterology* 2008;134:823–32.
  44. Duncan AW, Dorrell C, Grompe M. Stem cells and liver regeneration. *Gastroenterology* 2009;137:466–81.
  45. Liu M, Duke JL, Richter DJ, et al. Two levels of protection for the B cell genome during somatic hypermutation. *Nature* 2008;451:841–5.
  46. Rogozin IB, Pavlov YI, Bebenek K, et al. Somatic mutation hotspots correlate with DNA polymerase eta error spectrum. *Nat Immunol* 2001;2:530–36.
  47. Kato L, Begum NA, Burroughs AM, et al. Non-immunoglobulin target loci of activation-induced cytidine deaminase (AID) share unique features with immunoglobulin genes. *Proc Natl Acad Sci U S A* 2012;109:2479–84.

# Interleukin-1 and Tumor Necrosis Factor- $\alpha$ Trigger Restriction of Hepatitis B Virus Infection via a Cytidine Deaminase Activation-induced Cytidine Deaminase (AID)\*

Received for publication, July 12, 2013, and in revised form, September 8, 2013. Published, JBC Papers in Press, September 11, 2013, DOI 10.1074/jbc.M113.501122

Koichi Watashi<sup>‡1</sup>, Guoxin Liang<sup>§</sup>, Masashi Iwamoto<sup>¶</sup>, Hiroyuki Marusawa<sup>¶</sup>, Nanako Uchida<sup>‡</sup>, Takuji Daito<sup>‡</sup>, Kouichi Kitamura<sup>§</sup>, Masamichi Muramatsu<sup>§</sup>, Hirofumi Ohashi<sup>‡</sup>, Tomoko Kiyohara<sup>‡</sup>, Ryosuke Suzuki<sup>‡</sup>, Jisu Li<sup>||</sup>, Shuping Tong<sup>||</sup>, Yasuhito Tanaka<sup>\*\*</sup>, Kazumoto Murata<sup>††</sup>, Hideki Aizaki<sup>‡2</sup>, and Takaji Wakita<sup>‡</sup>

From the <sup>‡</sup>Department of Virology II, National Institute of Infectious Diseases, Tokyo 162-8640, Japan, the <sup>§</sup>Department of Molecular Genetics, Kanazawa University Graduate School of Medical Science, Kanazawa 920-8640, Japan, the <sup>¶</sup>Department of Gastroenterology and Hepatology, Kyoto University Graduate School of Medicine, Kyoto 606-8507, Japan, the <sup>||</sup>Liver Research Center Rhode Island Hospital, Warren Alpert School of Medicine, Brown University, Providence, Rhode Island 02903, the <sup>\*\*</sup>Department of Virology and Liver Unit, Nagoya City University Graduate School of Medicinal Sciences, Nagoya 467-8601, Japan, and the <sup>††</sup>Research Center for Hepatitis and Immunology, National Center for Global Health and Medicine, Ichikawa 272-8516, Japan

**Background:** Cytokines and host factors triggering innate immunity against hepatitis B virus (HBV) are not well understood.

**Results:** IL-1 and TNF $\alpha$  induced cytidine deaminase AID, an anti-HBV host factor, and reduced HBV infection into hepatocytes.

**Conclusion:** IL-1/TNF $\alpha$  reduced host susceptibility to HBV infection through AID up-regulation.

**Significance:** Proinflammatory cytokines modulate HBV infection through a novel innate immune pathway involving AID.

Virus infection is restricted by intracellular immune responses in host cells, and this is typically modulated by stimulation of cytokines. The cytokines and host factors that determine the host cell restriction against hepatitis B virus (HBV) infection are not well understood. We screened 36 cytokines and chemokines to determine which were able to reduce the susceptibility of HepaRG cells to HBV infection. Here, we found that pretreatment with IL-1 $\beta$  and TNF $\alpha$  remarkably reduced the host cell susceptibility to HBV infection. This effect was mediated by activation of the NF- $\kappa$ B signaling pathway. A cytidine deaminase, activation-induced cytidine deaminase (AID), was up-regulated by both IL-1 $\beta$  and TNF $\alpha$  in a variety of hepatocyte cell lines and primary human hepatocytes. Another deaminase APOBEC3G was not induced by these proinflammatory cytokines. Knockdown of AID expression impaired the anti-HBV effect of IL-1 $\beta$ , and overexpression of AID antagonized HBV infection, suggesting that AID was one of the responsible factors for the anti-HBV activity of IL-1/TNF $\alpha$ . Although AID induced hypermutation of HBV DNA, this activity was dispensable for the anti-

HBV activity. The antiviral effect of IL-1/TNF $\alpha$  was also observed on different HBV genotypes but not on hepatitis C virus. These results demonstrate that proinflammatory cytokines IL-1/TNF $\alpha$  trigger a novel antiviral mechanism involving AID to regulate host cell permissiveness to HBV infection.

The intracellular immune response can eliminate pathogens from a host, and host cells possess different mechanisms to counteract viral infection depending on the virus type. Human immunodeficiency virus (HIV) infection is restricted by cellular proteins designated as restriction factors, including APOBEC3G (A3G),<sup>3</sup> TRIM5 $\alpha$ , tetherin/BST-2, and SAMHD1 (1, 2). All of these factors can be induced by stimulation with interferon (IFN). Hepatitis C virus (HCV) is eliminated by type I and III IFNs derived from dendritic cells or infected hepatocytes (3–6). In hepatocytes, this process involves a series of antiviral factors that are downstream genes of IFN, IFN-stimulated genes (ISGs). Influenza virus spread and virulence is inhibited by cytokines such as IFNs and TNF $\alpha$ . Responsive genes for these mechanisms include IFN-induced cellular Mx proteins that are dynamin-like GTPases (7, 8). However, these cytokine-induced antiviral immune responses are poorly understood in hepatitis B virus (HBV) infection.

\* This work was supported by grants-in-aid from the Ministry of Health, Labor, and Welfare, Japan, the Ministry of Education, Culture, Sports, Science, and Technology, Japan, and the Japan Society for the Promotion of Science and incentive support from the Viral Hepatitis Research Foundation of Japan.

✂ Author's Choice—Final version full access.

<sup>1</sup> To whom correspondence may be addressed: Dept. of Virology II, National Institute of Infectious Diseases, Tokyo, 1-23-1 Toyama, Shinjuku-ku, Tokyo, 162-8640, Japan. Tel.: 81-3-5285-1111; Fax: 81-3-5285-1161; E-mail: kwatashi@nih.go.jp.

<sup>2</sup> To whom correspondence may be addressed: Dept. of Virology II, National Institute of Infectious Diseases, Tokyo, 1-23-1 Toyama, Shinjuku-ku, Tokyo, 162-8640, Japan. Tel.: 81-3-5285-1111; Fax: 81-3-5285-1161; E-mail: aizaki@nih.go.jp.

<sup>3</sup> The abbreviations used are: A3G, APOBEC3G; AID, activation-induced cytidine deaminase; HBV, hepatitis B virus; HCV, hepatitis C virus; ISG, IFN-stimulated gene; QNZ, 6-amino-4-(4-phenoxyphenylethylamino)quinazoline; GEq, genome equivalent; PHH, primary human hepatocyte; MTT, 3-(4,5-dimethylthiazol-2-yl)-2,5-diphenyltetrazolium bromide; ISRE, interferon sensitivity-responsive element; cccDNA, covalently closed circular DNA.

## Anti-HBV Activity of IL-1 and TNF $\alpha$ Mediated by AID

HBV infection is a worldwide health problem affecting more than 350 million people and is a major cause of the development of liver cirrhosis and hepatocellular carcinoma (9–11). During the course of infection, a number of cytokines and chemokines are up-regulated in HBV-infected patients, including IFN $\alpha$ / $\gamma$ / $\lambda$ , TNF $\alpha$ , IL-1, IL-6, IL-10, IL-12, IL-15, and IL-8 (12–15). Some of these cytokines are reported to suppress HBV replication (3, 16–21). In particular, type I, II, and III IFNs suppress the replication of HBV *in vitro* and *in vivo* (19, 20, 22–26). Although one of the downstream genes of IFN, A3G, has the potential to reduce HBV replication (27–34), it is still under discussion whether this protein is responsible for the anti-HBV activity of type I IFN, because it has been previously reported by Trono and co-workers (28, 35) that the induction of A3G does not explain the IFN-induced inhibition of HBV replication. Moreover, these studies were carried out using an HBV transgene that only reproduces a portion of the whole HBV life cycle, mainly focusing on intracellular HBV replication.

Here, we screened for cytokines and chemokines that affected HBV infection in HepaRG cells, a human hepatocyte cell line susceptible to HBV infection and reproducing the whole HBV life cycle (36, 37). IL-1 and TNF $\alpha$  decreased the host cell permissiveness to HBV infection, and this effect was at least partly mediated by the induction of activation-induced cytidine deaminase (AID). The anti-HBV activity of IL-1/TNF $\alpha$  was mechanistically different from that of IFN $\alpha$ . This study presents the activity of IL-1/TNF $\alpha$  to suppress HBV infection into hepatocytes independent of the effect on immune cells and the physiological role of AID in this machinery. Moreover, as far as we know, this is the first report to show the AID function to inhibit the infection of human pathogenic virus.

### EXPERIMENTAL PROCEDURES

**Reagents**—All cytokines were purchased from PeproTech or R & D Systems. Heparin was obtained from Mochida Pharmaceutical. Lamivudine, PD98059, SP600125, SB203580, and Bay11-7082 were obtained from Sigma. Entecavir was obtained from Santa Cruz Biotechnology. BMS-345541 and 6-amino-4-(4-phenoxyphenylethylamino)quinazoline (QNZ) were purchased from Merck.

**Cell Culture**—HepaRG cells (Biopredic) were cultured with Williams' medium E (Invitrogen) supplemented with 2 mM L-glutamine, 200 units/ml penicillin, 200  $\mu$ g/ml streptomycin, 10% FBS, 5  $\mu$ g/ml insulin (Wako), 20 ng/ml EGF (PeproTech), 50  $\mu$ M hydrocortisone (Sigma), and 2% DMSO (Sigma). HepG2, HepAD38 (kindly provided by Dr. Seeger at Fox Chase Cancer Center) (38), and HepG2.2.15 cells (a kind gift from Dr. Urban at Heidelberg University) (39) were cultured with DMEM/F-12 + GlutaMAX (Invitrogen) supplemented with 10 mM HEPES (Invitrogen), 200 units/ml penicillin, 200  $\mu$ g/ml streptomycin, 10% FBS, 50  $\mu$ M hydrocortisone, and 5  $\mu$ g/ml insulin in the presence (HepAD38 and HepG2.2.15) or absence (HepG2) of 400  $\mu$ g/ml G418 (Nacal Tesque). HepAD38 cells were cultured with 0.3  $\mu$ g/ml tetracycline when terminating HBV induction. Huh-7.5.1 cells (kindly provided from Dr. Chisari at Scripps Research Institute) were cultured as described previously (40). Primary human hepatocytes (PHH) isolated from urokinase-type plasminogen activator transgen-

ic/SCID mice inoculated with PHH (PhoenixBio) or purchased from Lonza were cultured with DMEM supplemented with 20 mM HEPES, 100 units/ml penicillin, 100  $\mu$ g/ml streptomycin, 10% FBS, and 44 mM NaHCO<sub>3</sub> or with 1 mM pyruvate, nonessential amino acids, 20 mM HEPES, 200 units/ml penicillin, 200  $\mu$ g/ml streptomycin, 10% FBS, 0.25  $\mu$ g/ml insulin (Wako), 5 ng/ml EGF, and 50 nM dexamethasone.

**HBV Preparation and Infection**—HBV used in this study was mainly derived from HepAD38 cells, which is classified as genotype D (38). Media from HepAD38 cells at days 7–31 post-induction of HBV by depletion of tetracycline were recovered every 3 days. Media were cleared through a 0.45- $\mu$ m filter and precipitated with 10% PEG8000 and 2.3% NaCl. The precipitates were washed and resuspended with medium at  $\sim$ 200-fold concentration. The HBV DNA was quantified by real time PCR. HBV genotype A and C in Fig. 7B was recovered from the media of HepG2 cells transfected with the plasmid pHBV/Acus and pHBV/C-AT (41).

HepaRG cells were infected with HBV at 2000 (Fig. 7B) or 6000 (other figures) genome equivalent (GEq)/cell in the presence of 4% PEG8000 for 16 h as described previously (36). Urban and co-workers (42) reported that more than  $10^3$  GEq/cell amount of HBV derived from HepAD38 or HepG2.2.15 cells (*i.e.*  $1.25$ – $40 \times 10^4$  GEq/cell) as inoculum was required for efficient infection into HepaRG cells. The anti-HBV effect of IL-1/TNF $\alpha$  shown in this study was also observed when inoculated with HBV at 300 GEq/cell (data not shown).

**Extraction of DNA and RNA**—HBV DNA was extracted from the cells or from the medium using a DNA kit (Qiagen) according to the manufacturer's protocol. Total RNA was recovered with RNeasy mini kit (Qiagen) according to the manufacturer's protocol.

**Real Time PCR and RT-PCR**—HBV DNA was quantified by real time PCR analysis using the primer set 5'-ACTCACC-AACCTCCTGTCT-3' and 5'-GACAAACGGGCAACAT-ACCT-3' and probe 5'-carboxyfluorescein (FAM)-TATCG-CTGGATGTGTCTGCGGCGT-carboxytetramethylrhodamine (TAMRA)-3' (43). The PCR was performed at 50 °C for 2 min, 94 °C for 10 min, and 50 cycles of 94 °C for 15 s and 60 °C for 1 min. Detection of cccDNA was achieved using 5'-CGTCTGTGCCTTCTCATCTGC-3' and 5'-GCACAG-CTTGAGGCTTGAA-3' as primers and 5'-CTGTAGGC-ATAAATTGGT (MGB)-3' as a probe (44). This primer-probe set theoretically detected neither relaxed circular DNA nor HBV DNA integrated into host genome but can capture cccDNA as described previously (44). For quantification of cellular mRNA, cDNA was synthesized from extracted RNA using SuperScriptIII (Invitrogen), followed by PCR with TaqMan Gene Expression Master Mix (Applied Biosystems) and primer-probe set (TaqMan Gene Expression Assay, Applied Biosystems) or with Power SYBR Green PCR Master Mix (Applied Biosystems) and 5'-AAATGTC-CGCTGGGCTAAGG-3' and 5'-GGAGGAAGAGCAATT-CCACGT-3' as primers for AID.

RT-PCR was performed as described previously (45) using a one-step RNA PCR kit (Takara). Primers for amplifying each gene were as follows: 5'-CTCTGAGGTTTAGCATTTC-3' and 5'-CTCCAGGTCCTCAAATGAATA-3' for *cIAP*; 5'-GCA-

GATTTATCAACGGCTTT-3' and 5'-CAGTTTTCCACCA-CAACAAA-3' for XIAP; 5'-TAGCCAACATGTCCTCACA-GAC-3' and 5'-TCTTCTACCACTGGTTTCATGC-3' for ISG56; 5'-GCCTTTTCATCCAAATGGAATTC-3' and 5'-GAAATCTGTTCTGGGCTCATG-3' for PKR; and 5'-CCATG-GAGAAGGCTGGGG-3' and 5'-CAAAGTTGTCATGGATG-ACC-3' for GAPDH, respectively.

**ELISA**—HBs protein was quantified by ELISA using plates incubated at 4 °C overnight with a sheep anti-HBs antibody at 1:5000 dilution (Maxisorp nunc-immuno plate, Nunc catalog no. 439454) followed by coating with 0.2% BSA, 0.02% Na<sub>2</sub>S<sub>2</sub>O<sub>3</sub>, 1× PBS at 4 °C until use. Samples were incubated with the plates for 2 h and after washing with TBST four times, horseradish peroxidase-labeled rabbit anti-HBs antibody was added for 2 h. The substrate solution (HCV core ELISA kit: Ortho) was reacted for 30 min before the A<sub>450</sub> values were measured.

**Indirect Immunofluorescence Analysis**—Indirect immunofluorescence analysis was performed essentially as described previously (45). After fixation with 4% paraformaldehyde and permeabilization with 0.3% Triton X-100, an anti-HBc antibody (DAKO, catalog no. B0586) was used as the primary antibody.

**MTT Assay**—The MTT assay was performed as described previously (46).

**Immunoblot Analysis**—Immunoblot analysis was performed as described previously (47). The polyclonal antibody against AID was generated using a peptide derived from AID protein as an immunogen as described previously for preparation of the anti-AID antibody 1 (48). The specificity of the antibody was described previously (48, 49).

**Lentiviral Vector-mediated Gene Transduction**—Lentivirus carrying shRNAs was prepared with 293T cells transfected with expression plasmids for HIV-1 Gag-Pol, VSV G, and shRNAs (sh-control, sh-cyclophilin A, sh-AID(1), sh-AID(2); Mission shRNA) (Sigma) with Lipofectamine 2000 (Invitrogen). Recovered lentiviral vector was transduced into HepaRG cells followed by selection with 1.5  $\mu$ g/ml puromycin. Lentivirus over-expressing AID, AID mutant, A3G, or the control lentivirus was recovered using expression plasmids for HIV-1 Gag-Pol, Rev, VSV G, and the corresponding expression vector as described previously (50).

**Southern Blot Analysis**—Southern blot was performed as described previously (41). After digestion of free nucleic acids with DNase I and RNase A, cell lysates were digested with proteinase K, and HBV DNA in the core particles was extracted with phenol/chloroform, followed by isopropyl alcohol precipitation. Probe was prepared by cutting pHBV/D-IND60 (41) with SacII and BspHI to generate a full-length HBV DNA probe and labeled with AlkPhos direct labeling reagents (GE Healthcare). Labeled bands were visualized with CDP-star detection reagent (GE Healthcare).

**Quantification of Nucleocapsid-associated HBV RNA**—After digestion of free nucleic acids with DNase I and RNase A, nucleocapsid was precipitated with PEG8000 (41). Total RNA was then extracted from the resuspended precipitates. HBV RNA was quantified by real time RT-PCR with 5'-TCC-CTCGCCTCGCAGACG-3' and 5'-GTTTCCCACCTTAT-

GAGTC-3' as primers with Power SYBR Green PCR Master Mix (Applied Biosystems).

**Co-immunoprecipitation Assay**—Co-immunoprecipitation assay was essentially performed as described (45).

**Differential DNA Denaturation PCR**—Differential DNA denaturation PCR was performed as described previously (51).

**Reporter Assay**—DNA transfection was performed with pNF- $\kappa$ B-luc or pISRE-TA-luc (Stratagene) and pRL-TK (Promega), which express firefly luciferase driven by NF- $\kappa$ B or ISRE and *Renilla* luciferase by herpes simplex virus thymidine kinase promoter, respectively, and Polyethylenimine Max (Polysciences Inc., catalog no. 24765). After compound or cytokine treatment, cells were lysed, and luciferase activities were measured as described previously (52). A reporter carrying HBV core promoter was constructed by inserting the DNA fragment (1413–1788 nucleotide number) of HBV DNA (D-IND60) into pGL4.28 vector (Promega) (41). In the reporter assay using this construct (Fig. 1H), HX531, a retinoid X receptor antagonist was used as a positive control as retinoid X receptor was involved in the transcription from the core promoter (53).

## RESULTS

**IL-1 Reduced Host Cell Susceptibility to HBV Infection**—To evaluate the effect of cytokines and chemokines on susceptibility to HBV infection, we treated HepaRG cells (36) with cytokines for 3 h prior to and 16 h during HBV infection, followed by culture without stimuli for an additional 12 days (Fig. 1A, lower scheme). Heparin, a competitive inhibitor of HBV attachment (54), was used as a positive control and decreased secretion of the viral envelope surface protein (HBs) from HBV-infected cells (Fig. 1A, upper graph, lane 38), which suggests a successful HBV infection in this experiment. Examination of 36 cytokines and chemokines revealed that IL-1 $\beta$  drastically decreased protein secretion from HBs (Fig. 1A, upper graph, lane 8). Although IFNs had a strong anti-HBV effect by a continuous treatment after HBV infection (Fig. 3C, panel b, and data not shown), they had only a limited effect in this screening where cytokines were only pretreated and cotreated with HBV (Fig. 1A, lanes 2–7). HBc protein expression (Fig. 1B) and HBV DNA (Fig. 1C) in the cells and medium (Fig. 1D) were significantly decreased by treatment with IL-1 $\beta$  without cytotoxicity (Fig. 1G). HBV cccDNA and HBV RNA was also decreased in infected cells treated with IL-1 $\beta$  (Fig. 1, E and F). IL-1 $\beta$  did not decrease HBV core promoter activity at least in HepG2 cells (Fig. 1H). These results suggest that IL-1 $\beta$  suppressed HBV infection to HepaRG cells. IL-1 $\beta$  did not decrease the expression of sodium taurocholate cotransporting polypeptide (NTCP), a recently reported HBV entry receptor (data not shown) (55). Similar results were obtained using primary human hepatocytes (Fig. 1I).

**NF- $\kappa$ B Signaling Was Critical for Anti-HBV Activity**—As shown in Fig. 2A, IL-1 $\beta$  suppressed HBV infection in a dose-dependent manner. This anti-HBV effect was reversed by cotreatment with a neutralizing antibody for the IL-1 receptor, IL-1RI (Fig. 2B), suggesting that receptor engagement was required for anti-HBV activity. IL-1Ra is a natural antagonist that associates with IL-1RI but does not trigger downstream signal transduc-

## Anti-HBV Activity of IL-1 and TNF $\alpha$ Mediated by AID

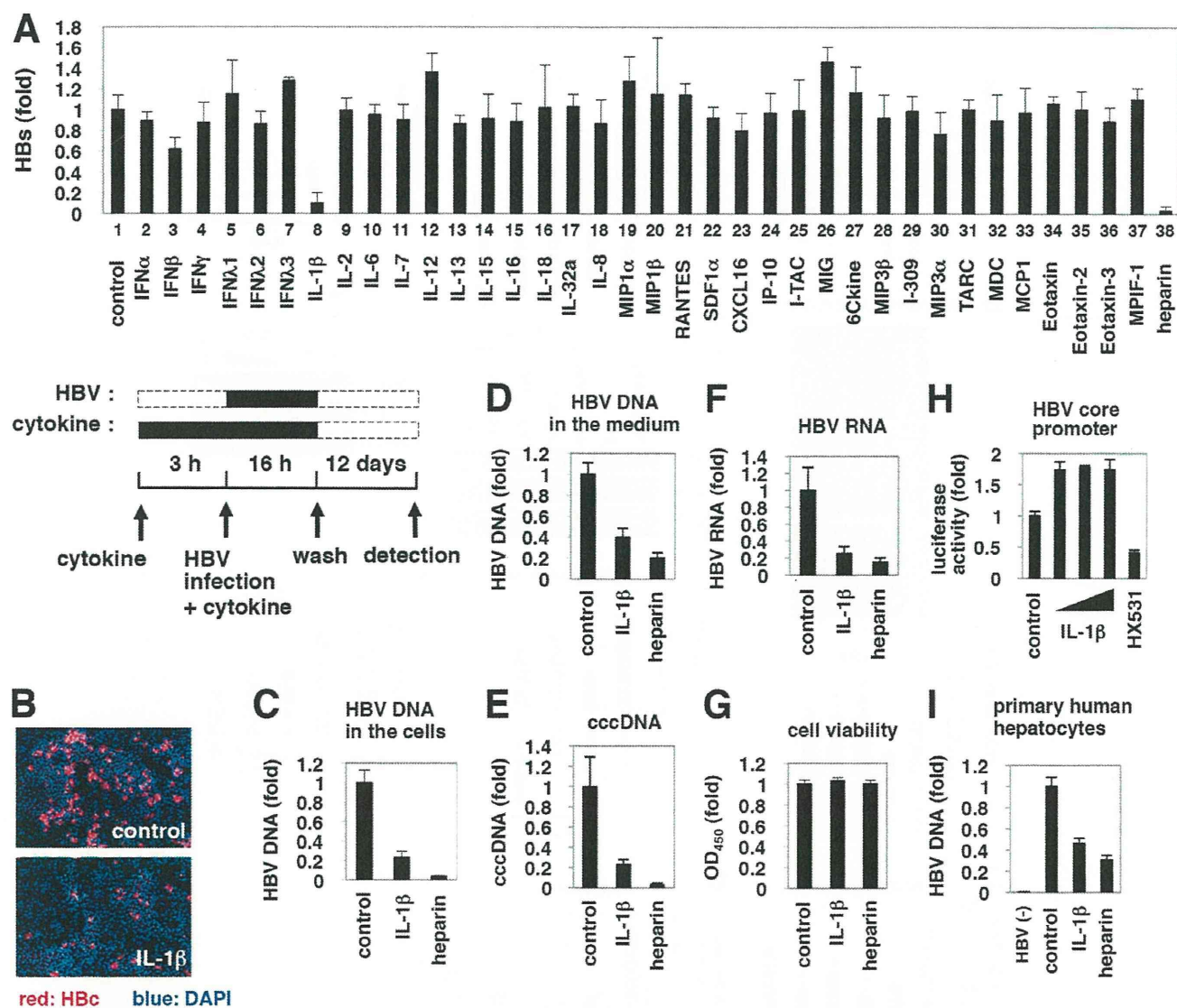


**FIGURE 1. Suppression of HBV infection by IL-1 $\beta$ .** *A*, upper graph, HepaRG cells were pretreated with cytokines at 100 ng/ml (except for IFN $\alpha$  and IFN $\beta$  at 100 IU/ml) or heparin at 25 units/ml as a positive control or were left untreated (*control*) for 3 h and then infected with HBV in the presence of each stimuli for 16 h. After washing, cells were cultured in normal growth medium for 12 days. HBs protein secreted into the medium was quantified by ELISA. Lower scheme indicates the treatment procedure for HepaRG cells. Black and dashed line boxes indicate the periods with and without treatment, respectively. *B–G* and *I*, HepaRG cells (*B–G*) or PHH (*I*) were treated as shown in *A* with or without 100 ng/ml IL-1 $\beta$  or 25 units/ml heparin as a positive control. HBc protein in the cells (red) was detected by indirect immunofluorescence analysis, and the nucleus was stained with DAPI (blue) at 12 days post-infection (*B*). HBV DNA (*C* and *I*), cccDNA (*E*), and HBV RNA (*F*) in the cells as well as HBV DNA in the medium (*D*) were detected. Cell viability was quantified by MTT assay (*G*). HBV(-) in *I* indicates uninfected cells. All of the data, except in *I*, are based on the average of three independent experiments. *I* shows the average results from one representative experiment, but the reproducibility of the data were confirmed in three independent experiments. *H*, reporter plasmid carrying the HBV core promoter was transfected with HepG2 cells and then treated with or without IL-1 $\beta$  (1, 10, and 100 ng/ml) and a retinoid X receptor antagonist HX531 as a positive control for 6 h. Luciferase activity was measured.

tion (56). Treatment with IL-1Ra did not decrease HBV infectivity (Fig. 2C), suggesting that signal transduction triggered by IL-1 was required for anti-HBV activity.

To identify the signal transduction pathway essential for anti-HBV activity, we treated HepaRG cells with PD98059, SP600125, SB203580, and Bay11-7082, which are inhibitors for MEK, JNK, p38, and NF- $\kappa$ B, respectively (57). As shown in Fig. 2D, only cotreatment with Bay11-7082 significantly removed the anti-HBV effect of IL-1 $\beta$ . Luciferase assay and RT-PCR analysis indicated that Bay11-7082, but not other inhibitors, blocked the transactivation of NF- $\kappa$ B (Fig. 2E, upper panels) and NF- $\kappa$ B downstream genes, *cIAP* and *XIAP* (Fig. 2E, lower

panels). Additional NF- $\kappa$ B inhibitors, BMS-345541 and QNZ (Fig. 2G), also reversed the anti-HBV effect of IL-1 $\beta$  (Fig. 2F). These data suggest a critical role for NF- $\kappa$ B activation in the anti-HBV activity. Additionally, IL-1 $\beta$  did not augment the activity of interferon sensitivity-responsive element (ISRE) and mRNAs for ISGs, *ISG56*, and double-stranded RNA-dependent protein kinase (*PKR*) in HepaRG cells (Fig. 2H), suggesting that the anti-HBV activity is independent of ISG up-regulation. TNF $\alpha$ , another cytokine that activates NF- $\kappa$ B signaling (Fig. 2E, lower panels), also inhibited HBV infection (Fig. 2I). Thus, NF- $\kappa$ B activation in host hepatocytes was critical for the anti-HBV activity of proinflammatory cytokines.

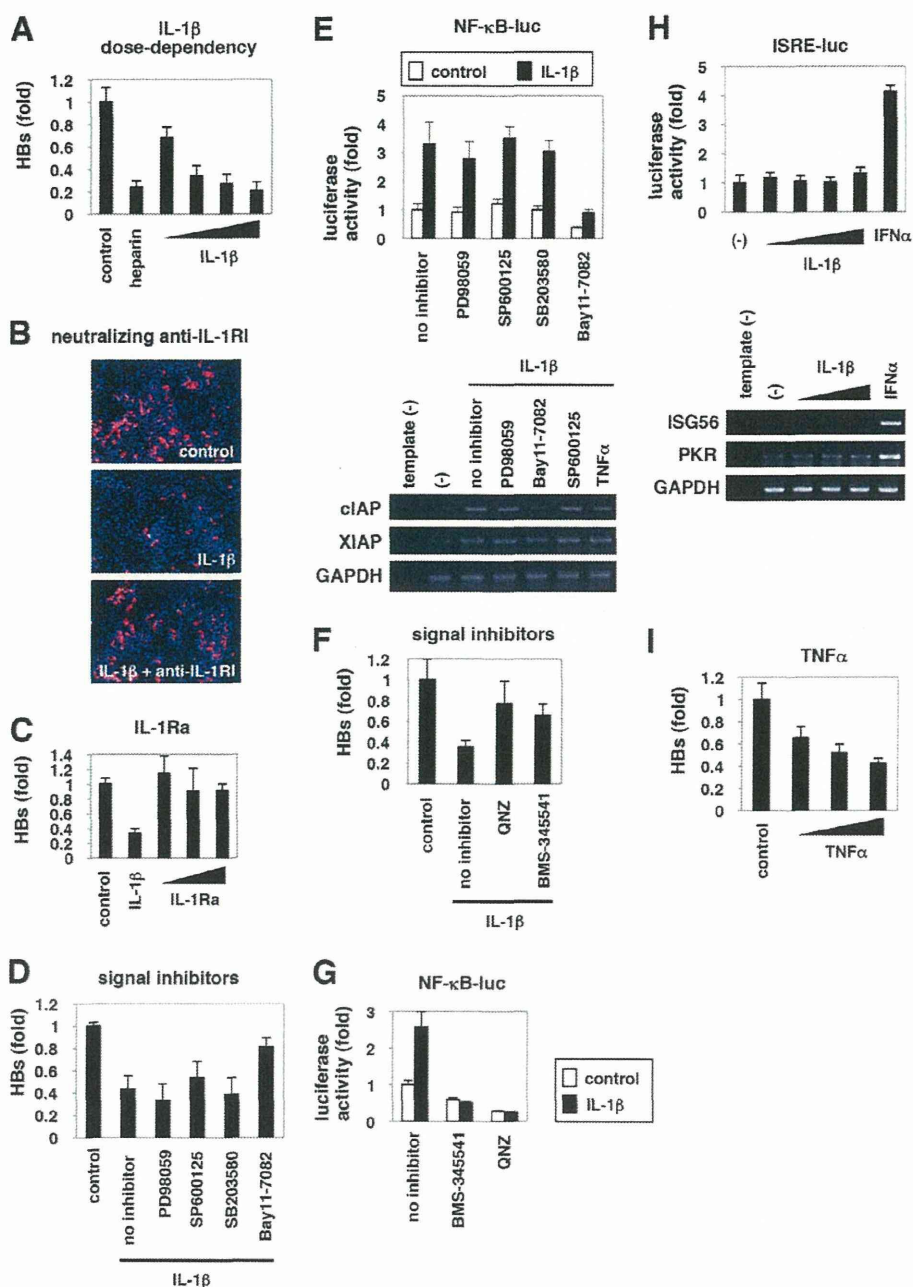


FIGURE 2. NF- $\kappa$ B activation triggered by IL-1 and TNF $\alpha$  was critical for anti-HBV activity. A–D, F, and I, HepaRG cells were left untreated (control) or treated with varying concentrations of IL-1 $\beta$  (1, 10, 30, and 100 ng/ml) or 25 units/ml heparin (A), with 30 ng/ml IL-1 $\beta$  together with or without a neutralizing anti-IL-1RI antibody at 20  $\mu$ g/ml (B), with 10 ng/ml IL-1 $\beta$  or varying concentrations of IL-1Ra (10, 30, and 100 ng/ml) (C), with 3 ng/ml IL-1 $\beta$  together with or without PD98059, SP600125, SB203580, or Bay11-7082 (D), or QNZ or BMS-345541 (F), or with TNF $\alpha$  (10, 100, and 300 ng/ml) (I) according to the treatment schedule shown in Fig. 1A. HBV infection was monitored by HBs protein secretion into the medium in A, C, D, F, and I and with Hbc protein in the cells in B, E, G, and H. NF- $\kappa$ B (E and G) and ISRE activity (H) were measured by reporter assay in the cells transfected with the reporter plasmid expressing luciferase driven from five tandem repeats of NF- $\kappa$ B elements (E, upper graph, and G) or ISRE (H, upper graph) or by RT-PCR in the cells (E and H, lower panels) upon signaling inhibitors used in D and F together with or without IL-1 $\beta$  (E and G), or upon IL-1 $\beta$  (10, 30, and 100 ng/ml) or IFN $\alpha$  100 IU/ml as a positive control (H) for 6 h. The white and black bars in the upper graph of E and G show the data in the absence or presence of IL-1 $\beta$ , respectively. Bands for mRNA for cIAP, XIAP, and GAPDH (E) or ISG56, PKR, and GAPDH (H) are presented in the lower panels. All of the data are based on averages of three independent experiments.

*Early Phase of HBV Infection as Well as HBV Replication Were Impaired by IL-1 Treatment*—Although heparin, an attachment inhibitor, could block HBV infection only if added together with the HBV inoculum, pretreatment with IL-1 $\beta$  before HBV infection was sufficient to show anti-HBV activity (Fig. 3A, panel b). This activity was amplified by a prolonged

treatment time of up to 12 h (Fig. 3B). Intriguingly, HBV cellular DNA was also reduced by IL-1 $\beta$  treatment following HBV infection (Fig. 3C, panel b). In contrast, IFN $\alpha$  was not effective by pretreatment (Figs. 3C, panel a, and 1A), although it did decrease HBV DNA by treatment after HBV infection (Fig. 3C, panel b), consistent with previous reports that IFN $\alpha$  can sup-